Bull. Mater. Sci., Vol. 31, No. 3, June 2008, pp. 441–447. © Indian Academy of Sciences.

Synthesis, characterization and electrochemical studies of $LiNi_{0.8}M_{0.2}O_2$ cathode material for rechargeable lithium batteries

R SATHIYAMOORTHI[†], P MANISANKAR[†], P SHAKKTHIVEL[††], MU SANG LEE and T VASUDEVAN*

Department of Chemistry Education, Teachers College, Kyungpook National University, Daegu 702-701, South Korea
[†]Department of Industrial Chemistry, Alagappa University, Karaikudi 630 003, India
[††]Department of Chemical Engineering, Yonsei University, Seodaemun-Ku, Seoul 120 749, South Korea

Abstract. **$LiNiO_2$ and substituted nickel oxides, $LiNi_{0.8}M_{0.2}O_2$ and $LiCo_{0.8}M_{0.2}O_2$ ($M = Mg^{2+}$, Ca^{2+}, Ba^{2+}), have been synthesized using simple solid state technique and used as cathode active materials for lithium rechargeable cells. Physical properties of the synthesized products are discussed in the structural (XRD, TEM, SEM with EDAX) and spectroscopic (FTIR) measurements. XRD results show that the compounds are similar to $LiNiO_2$ in structure. TEM and SEM analyses were used to examine the particle size, nature and morphological aspects of the synthesized oxides. The composition of the materials was explored by EDAX analysis. Electrochemical studies were carried out in the range 3–4·5 V (vs Li metal) using 1 M $LiBF_4$ in ethylene carbonate/dimethyl carbonate as the electrolyte. The doping involving 20% Mg resulted in a discharge capacity of 185 $mAhg^{-1}$ at 0·1 mA/cm^2 and remained stable even after 25 cycles. Discharge capacity retention for Mg doped lithium nickelate at 25th cycle was noted to be nearly 7% higher than for the undoped material.**

Keywords. **Lithium rechargeable cells; cathode material; TEM; nanoparticles; charge–discharge cycle; electrochemical properties.**

1. Introduction

In the last few years, lithium nickelate ($LiNiO_2$) has been considered as a promising positive electrode material for high energy rechargeable lithium–ion batteries (Thomas *et al* 1985; Dahn *et al* 1991; Broussely *et al* 1993, 1995; Ohzuku and Ueda 1994). However, because of its propensity for non-stoichiometry (Kanno *et al* 1994; Arai *et al* 1995; Rougier *et al* 1996), which strongly influences its electrochemical properties (Kanno *et al* 1994; Peres *et al* 1996; Rougier *et al* 1996), its thermal instability in the oxidized state (Dahn *et al* 1994; Ohzuku *et al* 1995; Arai *et al* 1998) and of the deterioration of its reversible behaviour upon cycling (Broussely *et al* 1995), an increasing research activity is now being devoted to new substituted $LiNi_{1-y}M_yO_2$ materials. Since, partial substitution for nickel can alter the structural and electrochemical properties of $LiNiO_2$, efforts to stabilize the two-dimensional (2*D*) layered structure of $LiNiO_2$, $LiNi_{1-y}M_yO_2$ phases (where M is a transition or a non-transition metal) with doping have been investigated (Morales *et al* 1990; Sathiyamoorthi and Vasudevan 2007a, b). The purpose of replacing/doping divalent nickel in the rhombohedral *R*-3*m* crystal structure of $LiNiO_2$ with some of the same sized divalent cations of alkaline earth metals is to improve cyclability, high voltage capacity and high temperature performance.

In this work, doping involving Mg, Ca and Ba metal ions with $LiNiO_2$ by solid-state reaction at a lower temperature of 600°C compared to the earlier works has been attempted with the aim of achieving higher capacity with minimum capacity loss on prolonged cycling at high voltage ranges of 3–4·5 V. By using simple solid-state reaction, a group of three different metal ions Mg^{2+}, Ca^{2+} and Ba^{2+} for nickel in $LiNiO_2$ were synthesized. Structural and morphological changes brought about by the addition of these metal ions in the $LiNiO_2$ matrix were investigated through surface examination techniques such as XRD, TEM and SEM. Electrochemical and charge retention properties were studied through cyclic voltammetry and charge–discharge studies.

2. Experimental

All the chemicals used were of E-Merck grade except graphite powder which was of Sisco brand. $LiNi_{0.8}M_{0.2}O_2$ (M = Mg, Ca and Ba) has been prepared using $LiNO_3$, $Ni(NO_3)_2$, $Mg(NO_3)_2$, $Ca(NO_3)_2$ and $Ba(NO_3)_2$ as precursor materials through low temperature solid-state reaction routine. The stoichiometric amounts of the precursors were weighed accurately and thoroughly mixed with three times of urea as fuel. 10% excess of $LiNO_3$ was added to avoid the loss of Li as Li_2O. During precursor material preparation, glycerol was used as the binding material (for every gram of the cathode material preparation 3 or 4

*Author for correspondence (drtvasudevan2002@yahoo.com)

drops of glycerol was used) which helped the mass of the ingredients to be brought into intimate mixing. A dark green colour paste material obtained was heated under air atmosphere in the furnace at 150°C for 2 h. Foam like mass of fly ash coloured material was obtained and it was crushed into a powdery form. The precursor samples were ignited at 600°C for 8 h for all the compositions of the cathode materials.

Electrochemical characterizations were performed in a 2016 coin cell-type two-electrode assembly. Cathode mix was prepared using 85% of the active material mixed with 10% acetylene black and 5% polyvinylidene difluoride (PVDF) in *N*-methyl-2-pyrrolidinone (NMP). The prepared mix was pressed onto an aluminium foil that serves as the current collector by applying 2 tons cm^{-2} pressure using a hydraulic press. Graphite was mixed with 5% of PVDF in NMP and pressed into a pellet. This was stored for a period of 24 h under vacuum atmosphere in presence of phosphorous pentoxide (P_2O_5) before use. Circular disks of the cathodes were then punched and were used for fabricating the coin cell. The coin-type cells were assembled in an argon-filled glove box with the prepared circular disks of $LiNi_{0.8}M_{0.2}O_2$ as cathode, graphite as anode, and with Celgard 2600 as separator in a non-aqueous electrolyte consisting of 1 M $LiBF_4$ in 50 : 50 by volume ethylene carbonate (EC)/dimethyl carbonate (DMC). The cyclic voltammetry technique was used to assess the topotactical reaction of lithium in the synthesized cathode materials. The cell with $LiNi_{0.8}M_{0.2}O_2$ (M = Mg, Ca and Ba) as working and lithium metal as reference and graphite as the counter electrode was cycled between 3 and 4·5 V at a scan rate of 0·1 mVs^{-1}. The cyclic voltammetry studies were carried out by using EG&G Instruments, PAR, Model 6310. Charge–discharge studies were performed at 0·1 $mAcm^{-2}$ in the voltage range 3–4·5 V using WPG 100 (Pontentiostat/Galvanostat) Won-A-Tech Instrument, South Korea.

The purity and structural properties of the synthesized products were investigated by JEOL (JDX-8030) X-ray diffraction analyser using Cu-Kα radiation. The FT–IR spectra were recorded for all the synthesized active cathode materials to confirm the expected moieties in the oxide material using Perkin Elmer FT–IR spectrophotometer in pressed KBr pellets. To analyse the particle nature, morphology and distribution of homogeneous size particles of the synthesized powders, scanning electron microscopic (SEM) photographs were taken by JEOL (JSM-840A) scanning electron microscope. The chemical compositions of the synthesized samples were confirmed by energy dispersive X-ray spectroscopic analysis (EDAX) using an X-ray detector attached to the SEM (Cambridge S-360) instrument. The transmission electron microscopic (TEM) analysis was performed for synthesized nanosized samples of lithium nickel based active cathode materials to find out the crystallization and particle size distribution using TEM JEOL JEM-2000 EX operated at 200 keV with point–to–point resolution of 2·3 Å.

3. Results and discussion

3.1 *XRD patterns*

Figure 1 presents the powder X-ray diffraction patterns of bare $LiNiO_2$, and alkaline earth metal doped $LiNiO_2$ at 600°C with incorporation of 20% for Ni in $LiNiO_2$ matrix. The XRD pattern of $LiNi_{0.8}M_{0.2}O_2$ (M = Mg, Ca and Ba) sample shows a well defined peak at $2\theta = 19°$ and the other less intensity peaks at 36° and 44°. The intensity vs diffraction angle peak data indicates the compound to crystallize in rhombohedral systems (space group, *R*3*m*) (Mohan Rao *et al* 2001). There are no additional peaks found which indicates the absence of unwanted phases. The lattice constants (computed from XRD data) were

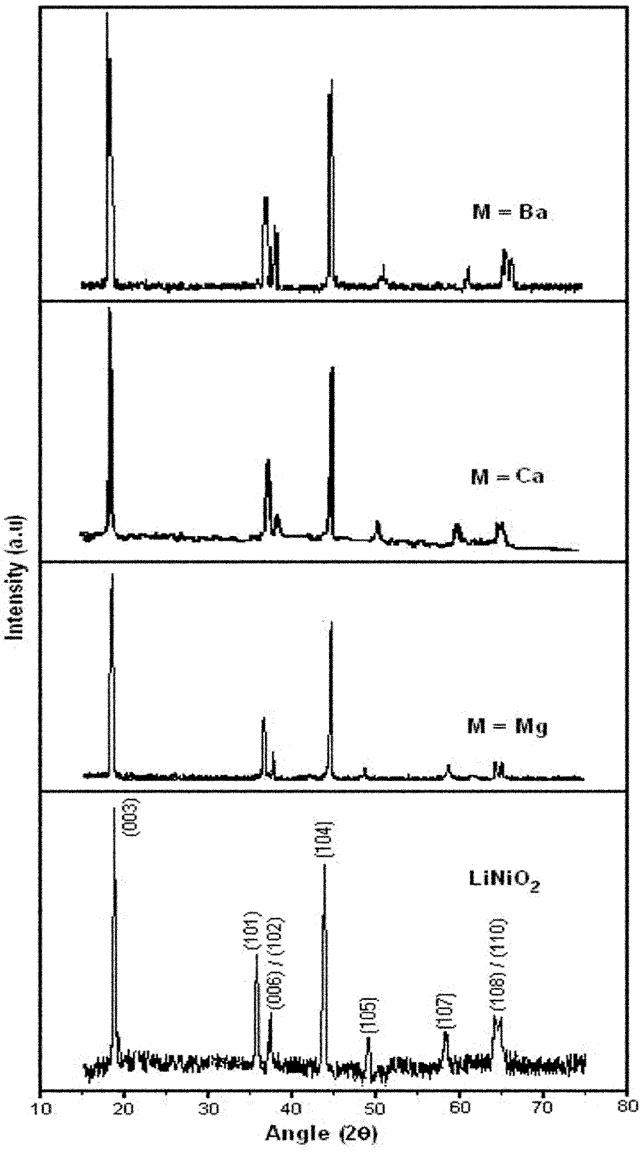

Figure 1. XRD pattern of $LiNiO_2$ and $LiNi_{0.8}M_{0.2}O_2$ (M = Mg, Ca and Ba).

Table 1. XRD lattice constants *a*, *c*, *c*/*a* ratio, unit cell volume and $I_{(003)}/I_{(104)}$ for $LiNiO_2$ and $LiNi_{0.8}M_{0.2}O_2$ (M = Mg, Ca and Ba).

Oxide material	*a* (Å)	*c* (Å)	*c*/*a*	Unit cell volume (Å)^3	$I_{(003)}/I_{(104)}$
Undoped $LiNiO_2$	2·8775	14·2144	4·9398	101·81	1·222
Mg doped $LiNiO_2$	2·8760	14·2169	4·9467	101·71	1·343
Ca doped $LiNiO_2$	2·8748	14·2182	4·9452	101·63	1·293
Ba doped $LiNiO_2$	2·8742	14·2229	4·9484	101·63	1·279

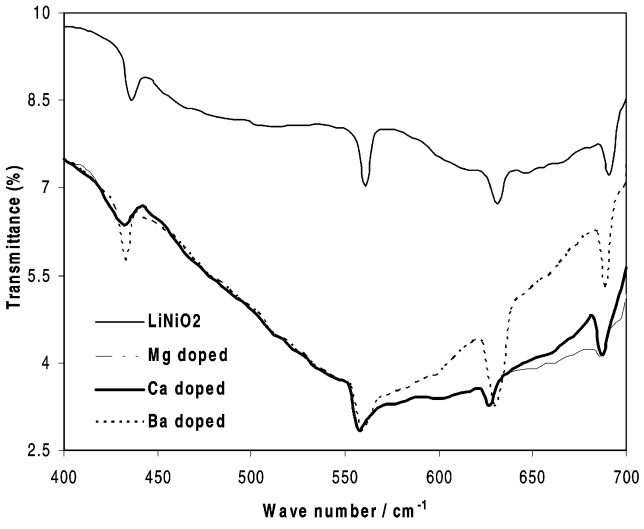

Figure 2. FTIR spectra of $LiNiO_2$ and $LiNi_{0.8}M_{0.2}O_2$ (M = Mg, Ca and Ba).

found to vary as a function of M^{2+} i.e. with the different dopants of M^{2+} for Ni in $LiNiO_2$, resulting in slight decrease in the lattice value '*a*' and increase in the '*c*' values. As a consequence unit cell volume decreased and the results are presented in table 1. A clear splitting of (006) (102) and (108) (110) doublets were observed for $LiNiO_2$ and at low concentration of Mg doping. As the Mg concentration is increased, (006) (102) and (108) (110) doublets tend to merge and the remaining peaks are slightly broadened, which is an indication of a reduced crystallite size coupled with microscopic strain in the crystal lattice. This could be due to a certain degree of mismatch in Mg^{2+} (0·66 Å) and Ni^{3+} (0·56 Å) ionic sizes.

These observations and the values of $I_{(003)}/I_{(104)} \approx 1{\cdot}22$ have been considered as a qualitative measure of better cathodic activity of the synthesized compounds (Morales *et al* 1990). Intensity ratios, $I_{(003)}/I_{(104)}$ value, indicates the enhanced stabilization of Ni^{3+} in the 2D-layered structure (Morales *et al* 1990) upon Mg substitution. Though the sizes of Ca^{2+} and Ba^{2+} ions are also not similar to that of Li^+, still these dopants are selected for the studies because of a few available encouraging results in the literature (Hasegawa *et al* 1997; Takanishi *et al* 1997; Kumta *et al* 2000). For every assigned (*hkl*) indices, lattice parameters are rightly assigned to compute constant values of the lattice parameters as least-square mean value of '*a*' and '*c*' in case of *hcp* or hexagonal and tetragonal crystal systems (Klug and Alexander 1967; Barrett and Massalski 1968; Azaroff and Buerger 1976; Cullity 1978). It is reported (Pouillerie *et al* 2000) for slightly Mg substituted lithium nickelates ($y \leq 0{\cdot}02$), that lithium deficiency required the presence of all Mg^{2+} ions in the inter-slab space. With ($y \leq 0{\cdot}2$), large amounts of Mg^{2+} ions were located at the lithium site. The presence of magnesium ions in the lithium site prevents any local collapse of the inter-slab space during the deintercalation process and this possibly could account for the arrest of capacity fading during prolonged cycling.

3.2 *FTIR spectral studies*

In addition to XRD experiments, further evidence for the formation of $LiNi_{0.8}M_{0.2}O_2$ (M = Mg, Ca and Ba) materials has been obtained from Fourier transform infrared spectroscopy (FT–IR) experimental data. According to the factor group analysis (Huang and Frech 1996; Prabakaran *et al* 1997), the infrared spectra of $LiMO_2$ (M = metals) compounds with *R*3*m* space group yield four infrared-active modes. Figure 2 represents the mode of vibrations for metal doped $LiNiO_2$ in the 400–700 cm^{-1} region which is largely associated with the vibrations of NiO_6 and LiO_6 octahedral units (Preudhomme and Torte 1972; Prabakaran *et al* 1997). The peaks at 627 cm^{-1} and 687 cm^{-1} are the vibration bending modes of NiO_6 i.e. ν[(Ni–O–Li)], the weak band around 432 cm^{-1} is assigned for the asymmetric stretching of Li–O in LiO_6 environments (Preudhomme and Tarte 1972; Prabakaran *et al* 1997).

In addition to these bands, a band at about 271 cm^{-1} in the far-IR region is expected (Zhecheva and Stoyanova 1993), but that region is not covered in the present study. As far as the low-waves peak is concerned, the isotopic replacement in $LiNiO_2$ has proved that this IR band between 200 and 300 cm^{-1} is associated with vibration of a relatively isolated LiO_6 octahedron (Tarte and Preudhomme 1970). The shape of IR absorption spectra remains the same as that of $LiNiO_2$, with a slight shift in the peaks towards lower frequency values showing that the local environment of lithium ions surrounded by oxygen anions is not affected and the NiO_2 layer covalency is

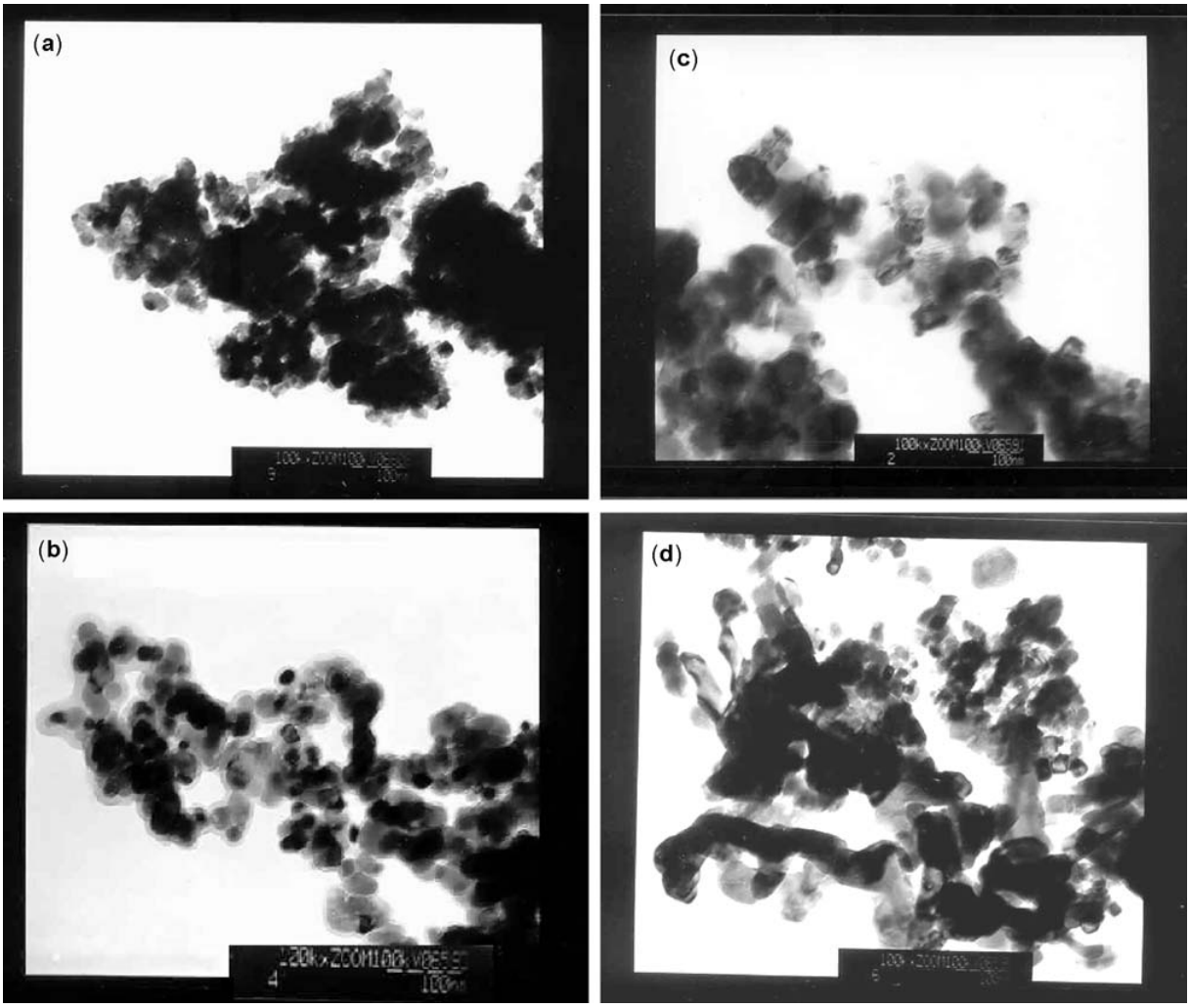

Figure 3. TEM photographs of (**a**) $LiNiO_2$, (**b**) $LiNi_{0.8}Mg_{0.2}O_2$, (**c**) $LiNi_{0.8}Ca_{0.2}O_2$ and (**d**) $LiNi_{0.8}Ba_{0.2}O_2$.

increased slightly (Julien *et al* 2000). At high level of magnesium substitution, the broadening of the infrared peaks can be interpreted as NiO_6 distortion due to magnesium induction in NiO_2 layers.

3.3 *Surface morphology and compositional analysis*

TEM photographs for undoped and metal doped $LiNiO_2$ synthesized at 600°C are presented in figure 3(a–d). In the case of undoped $LiNiO_2$, the cluster formation is ≈ 60 nm and also the particle size is little larger when compared with the Mg doped material, ≈ 40 nm. The interlayer distance may be higher with doped ones because of larger particle sizes. The surface area of the electrode material is an important characteristic parameter that determines the energy and power density of a particular battery system. In the present study, the surface area is expected to be higher for Mg doped cathode materials because of lesser particle size than other doped and undoped $LiNiO_2$.

SEM photographs taken for different alkaline earth metal doped and undoped synthesized lithium nickelates at two different magnifications are presented in figure 4(a–d). The figure shows that all the cathode materials are in nanometer particle size ranges. Among these, $LiNi_{0.8}Mg_{0.2}O_2$ is of lesser size in nature. We can expect the intercalation/deintercalation to be much easier in the $LiNi_{0.8}Mg_{0.2}O_2$, because of the reduced path length for lithium migration during charging–discharging process. As a consequence, higher capacity retention, cycle life and higher power density are to follow on.

EDAX studies have been carried out for the composition of synthesized metal doped $LiNiO_2$ nanoparticle cathode materials. The data show the presence of alkaline earth metal along with Ni with respect to the compositions prepared and the results are presented in table 2.

3.4 *Electrochemical properties*

Cyclic voltammograms of $LiNi_{0.8}M_{0.2}O_2$ (M = Mg, Ca and Ba) cells show the existence of reversible structure

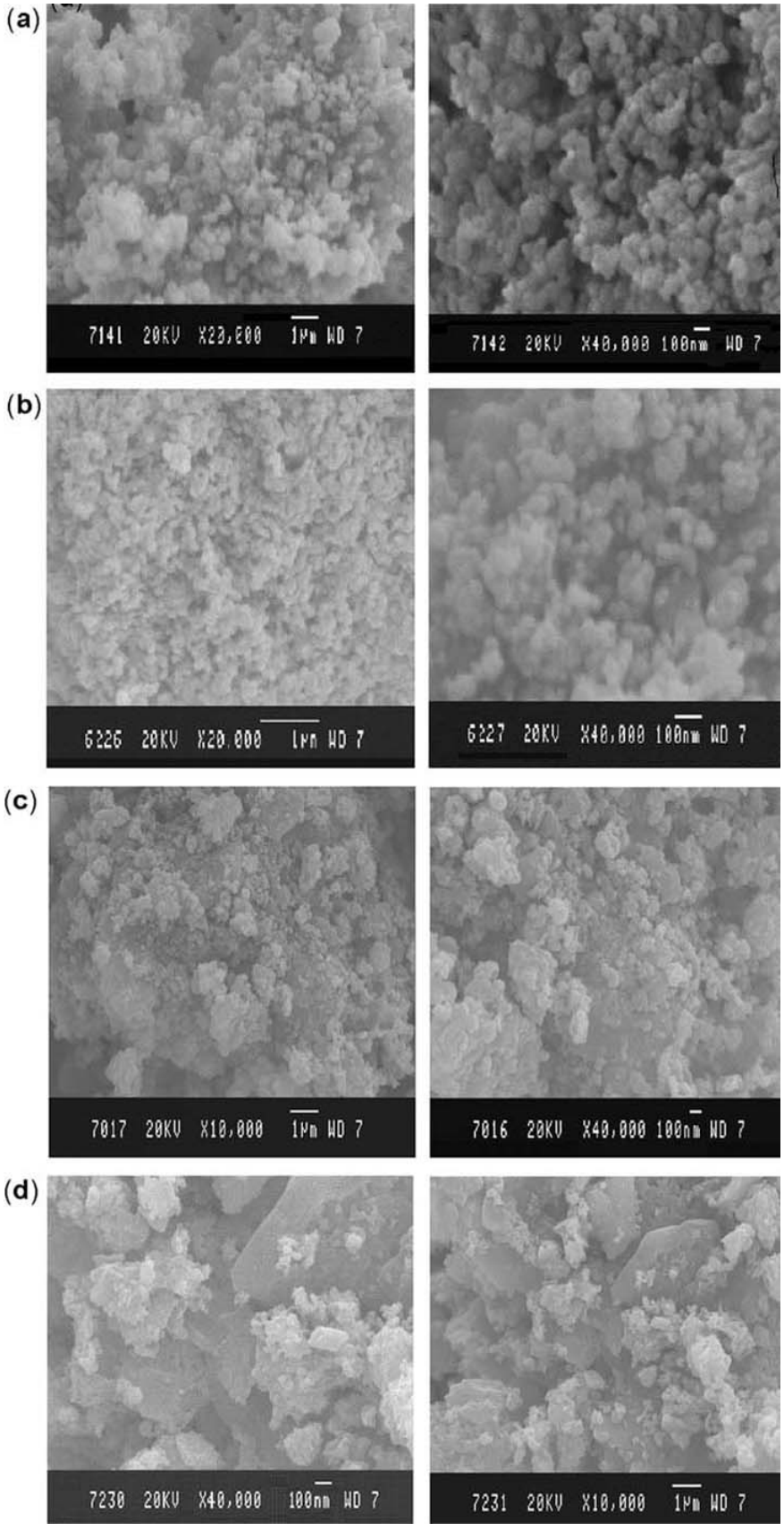

Figure 4. SEM photographs of (**a**) $LiNiO_2$, (**b**) $LiNi_{0.8}Mg_{0.2}O_2$, (**c**) $LiNi_{0.8}Ca_{0.2}O_2$ and (**d**) $LiNi_{0.8}Ba_{0.2}O_2$ at two different magnifications.

property by their redox activity as presented in figure 5. From the cyclic curves, the intercalation and de-intercalation of Li^+ over the range of 3–4·5 V were confirmed. Among these, the $LiNi_{0·8}Mg_{0·2}O_2$ has been observed to exhibit relatively narrower peaks with less peak separation compared to the voltammograms obtained with other materials. This indicates greater reversibility and redox activity for $LiNi_{0·8}Mg_{0·2}O_2$ material.

Table 2. EDAX composition analysis of $LiNi_{0·8}M_{0·2}O_2$ (M = Mg, Ca and Ba).

Sample	Nickel ratio (%)	Alkaline earth metal ratio (%)
$LiNi_{0·8}Mg_{0·2}O_2$	79·98	20·02
$LiNi_{0·8}Ca_{0·2}O_2$	80·23	19·77
$LiNi_{0·8}Ba_{0·2}O_2$	80·11	19·89

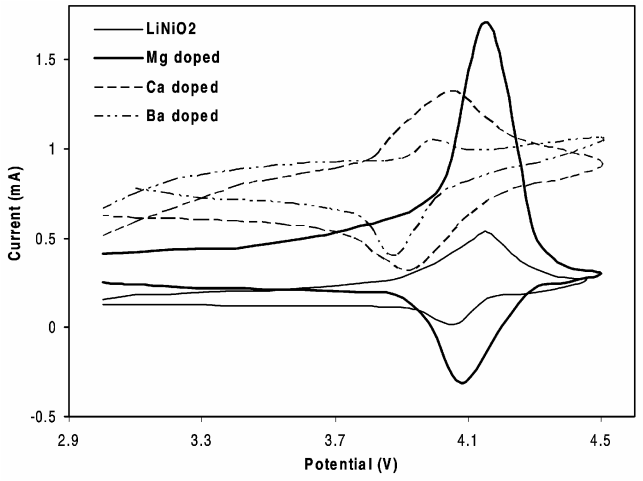

Figure 5. Cyclic voltammograms of $LiNiO_2$ and $LiNi_{0·8}M_{0·2}O_2$ (M = Mg, Ca and Ba).

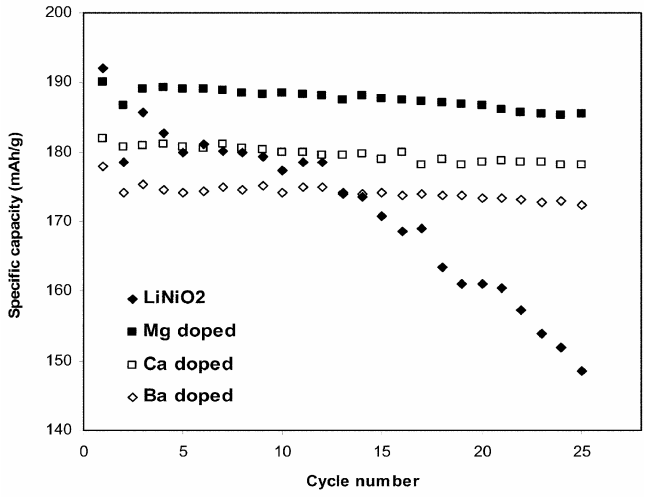

Figure 6. Plots of specific capacity vs cycle no. of $LiNiO_2$ and $LiNi_{0·8}M_{0·2}O_2$ (M = Mg, Ca and Ba).

To confirm the electrochemical performance by charge–discharge data, we cycled the fabricated 2016 lithium coin cell galvanostatically in the potential range 3–4·5 V. The first charge and discharge patterns for the cells incorporating the synthesized materials are presented in table 3. It is observed that the undoped $LiNiO_2$ (figure 6) has the first discharge capacity as 172 mAh g^{-1}, but, with Mg doping the first discharge capacity is found to be as high as 190 mAh g^{-1} and also the irreversible capacity being 13 mAh g^{-1} only. But, in the case of Ca and Ba doping in $LiNiO_2$, the first discharge capacities are noted to be 182 and 178 mAh g^{-1}, respectively. Having been encouraged by the preliminary performance of the synthesized powders, we were interested in carrying out the galvanostatic cycling studies up to 25 cycles so as to ascertain the stability of the initially observed capacity gains.

Figure 6 presents the cycling behaviour of the synthesized doped cathode materials in a lithium rechargeable 2016-type coin cell in the voltage range 3·5–4·5 V at a constant current density of 0·1 mA/cm^2. Excellent cyclability of Mg-doped material is exhibited over the investigated 25 cycles, i.e. there only being a difference of 4·6 mAh g^{-1} from the first to the 25th discharge capacities. This result seems to be interesting because of the stable, high voltage capacities realized. The enhanced performance of Mg doping cycling up to 4·25 V has been ascribed to enhanced electronic conductivity. $LiNi_{0·8}Mg_{0·2}O_2$ material exhibited around 98% discharge capacity retention at the end of 25th cycle compared to the undoped material. Presence of 20% Mg in the $LiCo_2O_2$ matrix, the capacity retention at 25th cycle is same as in $LiNi_{0·8}Mg_{0·2}O_2$ (97·6). But the reversible capacity is 191·3 mAh g^{-1} for $LiCo_{0·8}Mg_{0·2}O_2$ (inlcuded in table 3 for comparison) and for $LiNi_{0·8}Mg_{0·2}O_2$ it is 185·4 mAh g^{-1}. Thus, the capacity fading is very much arrested with doping of Mg. The cyclability of Ca and Ba-doped $LiNiO_2$ are around 178 mAh g^{-1} and 172 mAh g^{-1}, respectively at the end of 25th cycle. A comparison of the capacities of the present study with those of earlier results (Hasegawa *et al* 1997; Takanishi *et al* 1997; Kumta *et al* 2000) indicates the improved performance.

4. Conclusions

A simple low-temperature solid state reaction routine has been formulated to prepare $LiNi_{0·8}M_{0·2}O_2$ (M = Mg, Ca and Ba). The metal-doped $LiNiO_2$ materials synthesized by the present procedure results in enhanced electrochemical activity. Alkaline earth metal doped $LiNiO_2$ matrix shows that the particle sizes are in the range of 40–60 nm with highly ordered distribution. The capacity fading is less than 3% even after 25th cycle of charge–discharge studies with $LiNiO_2$ doped with alkaline earth

Table 3. Cathode charge–discharge and irreversible capacities of the compounds, $LiNiO_2$ and $LiNi_{0.8}M_{0.2}O_2$ (M = Mg, Ca and Ba).

Properties	$LiNiO_2$	$LiNi_{0.8}Mg_{0.2}O_2$	$LiNi_{0.8}Ca_{0.2}O_2$	$LiNi_{0.8}Ba_{0.2}O_2$
First charge capacity (mAh g^{-1})	197	203	202	198
First discharge capacity (mAh g^{-1})	172	190	182	178
Irreversible capacity for the 1st cycle (mAh g^{-1})	25	13	20	20
Reversible capacity in 25th cycle (mAhg^{-1})	157	185·4	178·1	172·3
Discharge capacity retention in 25th cycle (%)	91·3	97·6	97·9	96·7

metals. It has been demonstrated for the first time that the material, $LiNi_{0.8}Mg_{0.2}O_2$, is a promising high voltage (4·5 V) cycling cathode material with a delivering capacity of 185 mAh g^{-1} at 0·1 mA/cm^2 current drain for potential use in lithium rechargeable cells.

Acknowledgements

The authors gratefully acknowledge DST (NSTI), New Delhi, for the sanction of the research project. One of the authors (RS) thanks the DST (NSTI) for the award of a junior research fellowship and Prof. R Gangadharan, RMK Engineering College, Chennai.

References

Arai H, Okada S, Ohtsuka H, Ichimura M and Yamaki J 1995 *Solid State Ionics* **80** 261

Arai H, Okada S, Sakurai Y and Yamaki Y 1998 *Solid State Ionics* **109** 295

Azaroff L V and Buerger M J 1976 *The powder method* (McGraw Hill)

Barrett C and Massalski T B 1968 *Structure of metals* (Eurasia: McGraw Hill) 3rd ed

Broussely M, Perton F, Labat J, Staniewicz R J and Romero A 1993 *J. Power Sources* **43–44** 209

Broussely M *et al* 1995 *J. Power Sources* **54** 109

Cullity B D 1978 *Elements of X-ray diffraction* (Addison Wesley) 2nd ed

Dahn J R, Von Sacken U, Juzkow M W and Al-Janaby H 1991 *J. Electrochem. Soc.* **138** 2207

Dahn J R, Fuller E W, Obrovac M and Von Sacken U 1994 *Solid State Ionics* **69** 265

Hasegawa M, Bito Y, Ito S, Murata T and Toyoguchi Y 1997 U.S. Patent 5,631,105

Huang W W and Frech R 1996 *Solid State Ionics* **86–88** 395

Julien C, Nazri G A and Rougier A 2000 *Solid State Ionics* **135** 121

Kanno R, Kubo H, Kawamoto Y, Kamiyama T, Izumi F, Takeda Y and Takano M 1994 *J. Solid State Chem.* **110** 216

Klug H P and Alexander L E 1967 *X-ray diffraction procedure* (John Wiley)

Kumta P N, Chang C C and Sriram M A 2000 U.S. Patent 6,017,654

Mohan Rao M, Liebenow C, Jayalakshmi M, Wulff H, Guth U and Scholz F 2001 *J. Solid State Electrochem.* **5** 348

Moore R K and White W B 1970 *J. Am. Ceram. Soc.* **53** 679

Morales J, Vicente C P and Tirado J L 1990 *Mater. Res. Bull.* **25** 623

Ohzuku T and Ueda A 1994 *Solid State Ionics* **69** 201

Ohzuku T, Ueda A and Kouguchi M 1995 *J. Electrochem. Soc.* **142** 4033

Peres J P, Delmas C, Rougier A, Broussely M, Perton F, Biensan P and Willmann P 1996 *J. Phys. Chem. Solids* **57** 1057

Pouillerie C, Croguennec L, Biensan Ph, Willmann P and Delmas C 2000 *J. Electrochem. Soc.* **147** 2061

Prabakaran S R S, Michael M S, Radhakrishnan S and Julien C 1997 *J. Mater. Chem.* **7** 1791

Preudhomme J and Tarte P 1972 *Spectrochim. Acta* **A28** 69

Rougier A, Gravereau P and Delmas C 1996 *J. Electrochem. Soc.* **143** 1168

Sathiyamoorthi R and Vasudevan T 2007a *Electrochem. Commun.* **9** 416

Sathiyamoorthi R and Vasudevan T 2007b *Mater. Res. Bull.* (in press)

Takanishi K, Matsuda Y and Tsukamoto J 1997 U.S. Patent 5,679,481

Tarte P and Preudhomme J 1970 *J. Spectrochim. Acta* **A26** 747

Thomas M G S R, David W I F, Goodenough J B and Groves P 1985 *Mater. Res. Bull.* **20** 1137

Zhecheva E and Stoyanova R 1993 *Solid State Ionics* **66** 143